SEMARAK ILMU PUBLISHING

Journal of Advanced Research in Applied Sciences and Engineering Technology

Journal homepage:
https://semarakilmu.com.my/journals/index.php/applied_sciences_eng_tech/index
ISSN: 2462-1943

Multifunctional Double Band Mesh Antenna with Solar Cell Integration for Communications Purposes

Omar Raed Alobaidi[1,2,*], Mustafa Ghanim[3], Mustafa Thamir Wafeeq[4], Abdulmalek Ahmed Rija[2], Puvaneswaran Chelvanathan[5], Badariah Bais[1], Ameer Alhasan[6], Mohammad Hasan Basheet[7], Nowshad Amin[1]

[1] Department of Electrical Electronic & Systems Engineering, Faculty of Engineering & Built Environment, Universiti Kebangsaan Malaysia,43600 Bangi, Selangor, Malaysia
[2] Department of Electrical Engineering, College of Engineering, University of Anbar, Anbar 00964, Iraq
[3] Department of Communication Engineering, University of Technology, Iraq
[4] Information Technology Center, University of Technology, Iraq
[5] Solar Energy Research Institute, Universiti Kebangsaan Malaysia, 43600 Bangi, Selangor, Malaysia
[6] Department of Computer Techniques Engineering, Dijlah University College, Baghdad, Iraq
[7] Biomedical Engineering Department, Engineering College, Al-Nahrain University, Jadriah, Baghdad, Iraq

ABSTRACT

A dual band flexible antenna based on a circularly polarized modified meshed patch antenna design. This article focuses on some of the most pressing issues in small satellite applications. The antenna optimization and improvement of antenna performance, such as radiation efficiency. As is well known, circular polarization is immune to the Faraday rotation effect in the ionosphere and can thus prevent a 3-dB loss in geo-satellite communication. With the use of the software program Computer Simulation Technology (CST), the proposed circularly polarized modified meshed patch antenna has been created. Therefore, this article also presents a modified design of a circularly polarized meshed patch antenna to reduce the complexity of the antenna and decrease the size as much as it is capable. However, a meshed patch antenna can support a high communication data rate. The antenna architecture will theoretically be consistent with the installation of solar panels. The antenna utilizes a conductive copper as the core material and the substrate using flexible polyimide. The design antenna is very small, having an overall size of 30 * 30 mm when compared to other conventional non-transparent antenna operating at the same frequencies of 2.6, 3.5 GHz. The antenna that is proposed involves two meshed patch elements of same size but in various shapes. Finally, the proposed antenna is integrated into a solar cell by using the amorphous silicon thin film.

Keywords:

Transparent antenna; Mesh antenna; Solar cell; Flexible; 5G; Polyimide

1. Introduction

Optically transparent conductors have revolutionized electronics in many [1,2], televisions [3], laptops [4,5], smartphones [6,7], smartwatches [8] and solar panels [9,10]. These conductors are

* *Corresponding author.*
E-mail address: omar.raed@uoanbar.edu.iq

https://doi.org/10.37934/araset.54.1.294312

materials that allow light to pass through while also providing electrical conductivity. Translucent films (TCFs), the most common optically transparent conductors, are used in a variety of applications, including handheld touch screens and flat-panel TVs [11,12].

Translucent films (TCFs), the most common optically transparent conductors, are used in a variety of applications, including handheld touch screens and flat-panel TVs [11,12]. Because these deposited thin films in the visible spectrum are normally translucent, they can be deposited (mounted) on aircraft windows to provide electromagnetic interference (EMI) shielding from aircraft electronics. These materials are typically used in applications where optical clarity is needed because the material (visible speed clarity) must be easily seen by a person and conductivity requirements are restricted because most applications are low frequency [13]. However, the development of multimodal data mergers [14,15], the growth in CubeSats [16-18] and the beginning of a drone [19-21] have put pressure on sensor developers to increase payload effectiveness while minimizing scale, weight, and power, among other enhancements (SWaP). Antennas with high efficiency optically translucent drivers can be used for single-aperture lidar-radar fusion for autonomous vehicle navigation. On CubeSat missions, as antenna communication and sensing, and on camera-lens, integrated antennas for visible and thermal imaging. The technologies and history of optically translucent conductors have paved the way for products such as transparent microwave antennas, connectors, filters, and millimetre-wave (mm-wave) devices. Micro- and mm-wave frequency conductors that are optically transparent allow previously unattainable modern fusion processes and electromagnetic systems. Many studies have been conducted to evaluate the suitability of integrated antennas or translucent antennas with solar cells for a variety of applications, like Wi-Fi [22], x-band satellite [23], RFID radio frequency identification (RFID) [24] and indoor applications [25], emerging applications [26], outdoor applications [27], satellite communications [28-31], CubeSat applications [32,33], solar cell application [34-36], Bluetooth antenna communication [37], 12 GHz applications [38] and small satellites [16,39], satellite and terrestrial applications [40], CubeSat deployment [41]. We find in the literature some articles show and talk about some effect between the antenna and the solar cell [30,33,34]. The future of wireless communication depends on the system and its ability to operate autonomously. One common method is to power the system with electricity from various sources. However, sources may have several drawbacks, including high costs for maintenance and repair, and being environmentally unfriendly. Reliable sources that are cost effective, environmentally friendly, and require little maintenance are in high demand. One of these sources is a solar panel which has been used to power the wireless communication system by combining it with a solar panel and a transparent antenna system. This integration, however, has resulted in a slew of issues and difficulties that can be categorized into many categories. The first category is related to performance. Integrating antennas with solar cells doesn't impair performance, posing a primary challenge [36,40]. The second category is concerned with materials. An opaque metallic antenna casts shade on the photovoltaic cells, which can obstruct the solar cells' access to light [34]. Because most of the flexible antennas illustrated in the literature were made of non-transparent conductors such as copper, silver, and gold, placing them on an electrical circuit (e.g., solar cell) will minimize system efficiency and degrade system functionality [42]. The third category is concerned with design. Most methods are inapplicable for meshed patch antennas combined with solar panels because of their unique properties [32]. Although integration of antennas with amorphous (a-Si) and crystalline (c-Si) silicon solar cells has been reported, reducing antenna footprints and solar shadowing associated designs remain difficulties [26]. T The fourth category is size, which refers to small satellites restricted surface area. Because of their size and weight, the surface area of antennas, test instruments, and solar cells may affect satellites. The ability to fully exploit a small

satellite's limited surface area is a significant challenge. Transparent antennas are typically designed to optimize the solar panel surface area, which is critical for effective solar power harvesting and the space vehicle's ability to operate for an extended period [16,38]. The last category of challenge is combining solar cells, antennas, and other components deployed in small spaces, such as CubeSats or even smaller satellites. Integrating optically transparent antennas with solar cells [37,39,41,43] is one of the most difficult difficulties in installing wireless sensor nodes in contemporary environments since most small sensor nodes are battery powered [37]. In this article, a circularly polarized modified meshed patch antenna design is introduced for small satellite applications using the Computer Simulation Technology (CST) software. The suggested antenna produces 2.6, 3.5 GHz frequency bands. The antenna uses conductive copper as the core material and the substrate using flexible polyimide. The design antenna is tiny and flexible, having an overall size of 30 mm * 30 mm when compared to other conventional non-transparent antenna operating at the same frequencies. The antenna that is proposed involves two meshed patch elements of same sizes but in various shapes. Hence, it is of huge importance in small satellites and many other applications. The Antenna simulations are analysed based on production and measurements. As stated in Table 1, the output of the antenna, particularly the transparency, efficiency, flexibility, and gain, is unique for the recommended band of applications.

Table 1
Comparison between the proposed design and other mesh or transparent antennas from the literature

Reference	Technology used	Frequency (GHz)	GAIN (dB)	Efficiency (%)	Transparency (%)	With solar cell	Cost	Flexibility
[44]	Copper	30	20	-	-	no	low	inflexible
[35]	ITO	26	22.2	-	~ 100	no	high	inflexible
[45]	Cross dipoles	20	26.3		≥ 60	yes	medium	inflexible
[46]	Copper foils	20	27.3	65.9	81	yes	high	inflexible
[47]	Wired metal mesh (WMM)/micro metal mesh films (μmmf)	2.2/2.4	4.1/5.2	56.8/50.9	82.6/68.6	no	medium	inflexible
[48]	Fused quartz	56.3	9.55	-	74.6	no	high	inflexible
[49]	Meshed antenna	2.5	4.7	-	94	yes	medium	inflexible
[50]	Double-sided micrometric mesh metal	58	13.6	60	68/87	no	medium	inflexible
[51]	Soda lime glass substrate with gallium doped zinc oxide (GZO) thin film	5.2	3.04	-	98.0%	yes	low	inflexible
[43]	ITO-copper,	10	15	65	90	yes	low	inflexible
This work	Polyimide- copper	2.6 / 3.5	3.3	81.5	95	yes	low	flexible

2. Antenna Design

We will present the concept of the antenna; the antenna architecture will theoretically be consistent with the installation of solar panels so the antenna can be used for solar application. We will show how to design an antenna to increase the performances of the antenna, especially in radiation efficiency and the gains of which are important and should be studied. First, a modified meshed shape a resonator. Then, proximity coupled with feeding technique applies to feed the antenna. Research flow chart is shown in Figure 1.

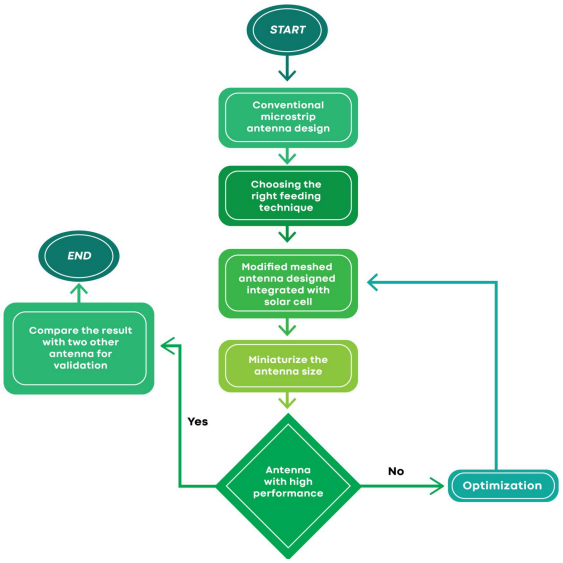

Fig. 1. Flow Chart of Research

2.1 Proximity-Fed Square Patch (Capacitive and Inductive)

In prior studies, it is shown that the coplanar proximity became the basis of the proposed design is because it bears a microstrip line that is open-ended [52]. According to the literature review, this type of feeding technique has been presented with the capacitive and inductive coupling as two various coupling mechanisms. An example has been shown in (Figure 2a) of a square shaped patch with capacitive coupling whereby the square patch central line is placed from the tip (T) of the open-ended feed line at a half wavelength. The feed lines voltage standing wave has a magnitude limit that corresponds to the patch canter, and the coupling across the gap results in a basic resonant current pattern (shown by the arrows in Figure 2b(i)) that runs perpendicular to the feed line, showing linearly polarized radiation in the far field. The square patch edge is aligned with the feed lines tip with inductive coupling (Figure 2b (ii)). The patch is driven by the current standing waves magnitude limit, which is 90 degrees out of phase with the voltage standing wave. Both the patch electromagnetic polarization and surface current are orthogonal to their capacitive coupling counterparts. Two techniques of the proximity feed can be used for meshed square patches, as shown in Figure 6. To facilitate the desired polarization while suppressing the antennas cross-polarization level, the number of current carrier lines (the ones making paths for the resonant currents) in the meshed patch can be made greater than equipotential lines (the ones only responsible for cross-connecting current carrier lines).

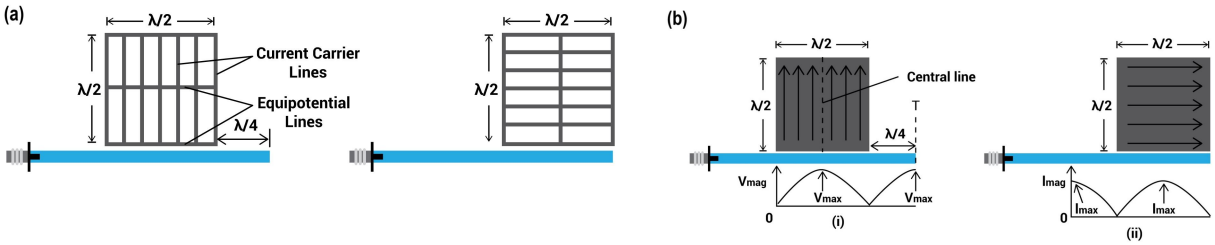

Fig. 2. Capacitive and inductive proxy coupling mechanism (redrawn from ref [51,52])

2.3 Antenna Design (Circular Polarization Design)

The two meshed patch antennas in Figure 2 radiate two linear polarizations that are orthogonal to each other. Given that the two-component patches resonate at slightly different frequencies, the suggested mesh antenna for CP, shown in Figure 3, can be made by merging these two antennas into a more compact configuration without changing their polarization directions.

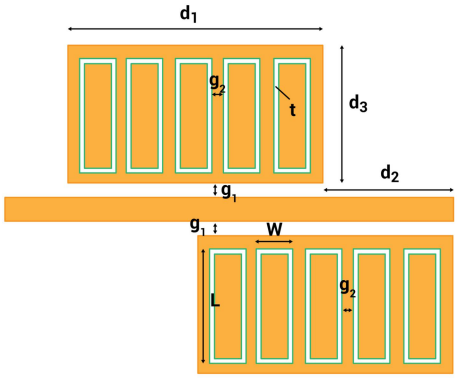

Fig. 3. Shrank size of proposed antenna

The common feed line design enables the ability to serve the two patches of the two types of coupling methods mentioned before. With an increase in voltage magnitude and a decrease in current magnitude, as theoretically illustrated in Figure 4. are created along the open-ended feed line, the feed line current generates decreasing currents, via inductive coupling, on the patch below the feed line (showed with black arrows in Figure 4). Simultaneously, the feed line's voltage forms the decrease of surface currents, through capacitive coupling, flowing from the gap side towards the opposite end of the other patch (showed with black arrows in Figure 4). Hence, the two patches' currents emerge in phase if the two patches resonate at the same frequency. Thus, both patches should resonate at two frequencies that differ slightly from one another.

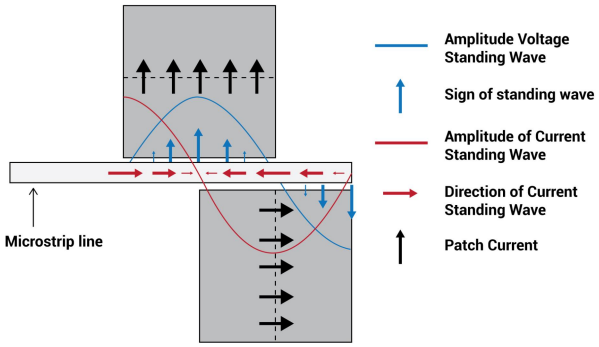

Fig. 4. A meshed antenna circularly polarization details (redrawn from ref [53])

As a result, through the antenna configuration, a CP can be got as illustrated in Figure 3, by cautiously altering the two patches size in a way which their resonant frequencies differences between would cause a required phase difference [54]. Referring to the structure in Figure 2. a higher frequency resonation of the capacitively coupled patch can accomplish a left-handed circular

polarization (LHCP), while a higher frequency resonation of the inductively coupled patch can produce a right-handed circular polarization (RHCP).

2.5 Modified Meshed Cp Proposed Antenna

The proposed antenna is designed step by step as follows Figure 5.

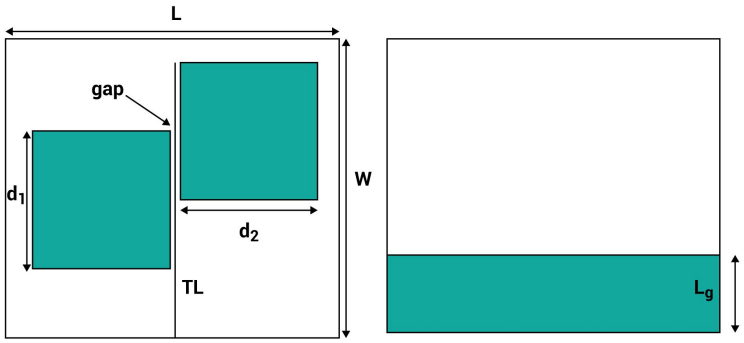

Fig. 5. The $\lambda/2$ dimension Cap & Ind of normal CP antenna (front view (a), ground view (b))

Table 2 shows the normal CP patch antenna. After designing the conventional rectangular microstrip antenna, decreasing the antenna dimensions comes to mind. Thus, the dimensions of the antenna have been optimized and shrunk compared to the wavelength.

Table 2
The shrank size of CP normal patch antenna dimensions

Parameters	Dimension(mm)
L	125
W	140
TL length	115
TL width	0.5
d_1	57.5
d_2	57.5
GND length (Lg)	32.89
Gap	1

Then the patch width for both the capacitive (Cap) and inductive (Ind) part decreased to $d_3 = \lambda/4$, which can be seen in Figure 6.

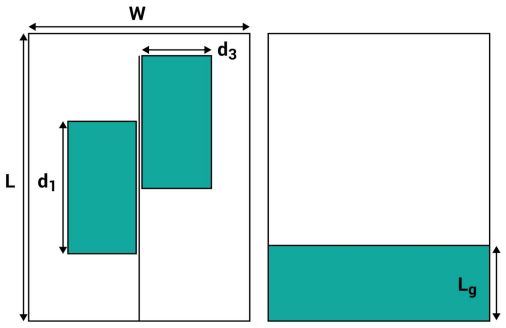

Fig. 6. CP normal patch antenna shrinking size

The dimensions of this antenna showed in Table 3.

Table 3
The shrank size of CP normal patch antenna dimensions

Parameters	Dimension(mm)
L	125
W	90
d_1	57.5
d_2	57.5
Lg	32.89

In addition, the applied substrate for the proposed antenna as a transparent antenna is a polyamide with permittivity of 2.6, and loss tangent of 0.0027, and thickness of the 0.1 mm and metallic part for this antenna is copper because of having a good conductivity [54,55]. Copper has been chosen for the metallic part to compensate for the loss which is produced by the substrate. The great deal for this type of antenna is low efficiency happens because of the significant loss of substrate. Shrinking the antenna dimensions is another reason for decreasing the antenna efficiency. Hence, reducing the antenna dimensions and increasing the efficiency of the antenna as performance should be considered simultaneously. The dimensions of the antenna are still too big to meet the application requirements. Thus, it should be shrunk more. So, the patch length and width for both Cap and Ind parts decreased to $d_4 = \lambda/4$ and $d_5 = \lambda/8$, respectively; then is optimized to get the exact resonance. The substrate dimensions of the antenna will reduce, though Figure 7.

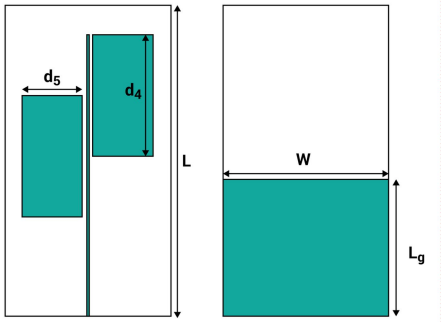

Fig. 7. The shrank size of CP normal patch antenna to $\lambda/4$ length patch

The dimensions of this antenna showed in Table 4. To achieve the exact resonance, the resonance frequency can be shifted by optimizing either the patch dimensions or ground length or even both.

Table 4
The shrank size of CP normal patch antenna dimension

Parameters	Dimension(mm)
L	75
W	40
d_1	29
d_2	14.5
Lg	12

According to the results that have been got from the previous antenna, the efficiency and the gain of the antenna are still low and couldn't meet our application requirements and the antenna dimensions must be shrunk as much as it could be. But decreasing the antenna dimensions causes the efficiency decrement, so the total thickness of the antenna has been increased and change to a multi-layer compacted antenna [56]. A super glue layer with a permittivity of ε_r= 3.3 can even paste the second layer to the first one. Therefore, a tetra ethylene substrate has been added to the antenna as a second layer with permittivity of 2.08 and thickness of 0.25 mm with just a ground layer to increase the efficiency and even the gain of the antenna and the antenna dimensions have been reduced simultaneously [57]. Figure 8 shows the prototype of the new antenna.

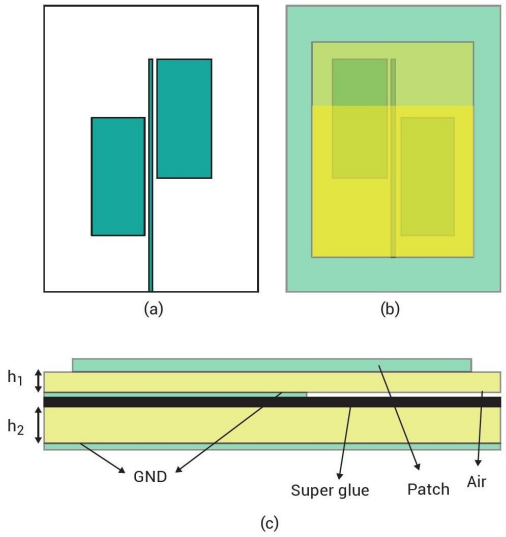

Fig. 8. Prototype of the antenna (a) Front view (b) Super glue prototype (c) Side view

Figure 8 shows the prototype of the antenna which contains:

i. the front view of the antenna by dimensions of 53.5 × 40 mm
ii. the super glue layer which has been cut due to be considered as a mixture with air
iii. demonstrates the side view of the antenna.

By changing the dimensions of the patch and the first GND, the resonating frequency of the antenna can be shifted to both higher and lower frequency band. The second layer can play the same role either. For instance, increasing the thickness will shift it to the higher and reducing it will shift it to the lower frequencies. Next step is adding a modified meshed shaped which has been cut from both Cap and Ind parts with the same dimensions to increase the antenna performances. The newly shaped has been changed to reduce the complexity of the antenna in low profile and because of the fabrication limitations. The new shape of the antenna can be shown in Figure 9. To meet the purpose of miniaturizing the antenna dimensions and make it small. The new dimension is 50 × 30 mm and for the parts can be referred to the Figure 9.

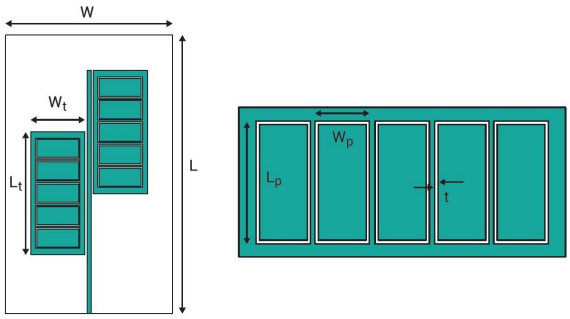

Fig. 9. The modified meshed CP antenna

Table 5 shows the modified meshed CP antenna dimensions.

Table 5
The modified meshed CP antenna dimensions

Parameters	Dimension(mm)
L	50
W	30
t	0.5
W_t	10
L_t	22
W_p	3.6
L_p	8.2

Based on the results for this antenna, the resonant frequency has been achieved, but the gain and efficiency of the antenna are still low. This loss in performance happens because of the fringing fields, the tangent loss of the substrate and the surface current. Another reason is the thickness of the antenna, which is too low compared to wavelength. One way to increase the antenna's efficiency would be to increase the substrate thickness, although it will also enhance the electric field around the edge of the antenna. Thus, some slots should be cut from the ground of the second substrate to reduce this undesired electric fields [58,59]. According to the microstrip slot antenna principles which mentioned in the literature review, the antenna's efficiency and gain can be amplified by cutting its ground. Following the approach of cutting the antenna ground on the second substrate, the current surface and electric density of the antenna should be known and located first. Figure 10. Shows the current surface and the electric fields distribution line. By knowing their density location, we can locate the slot next to them to reduce the current density. Before cutting the ground, the dimensions have been reduced to 30 × 30 mm [60].

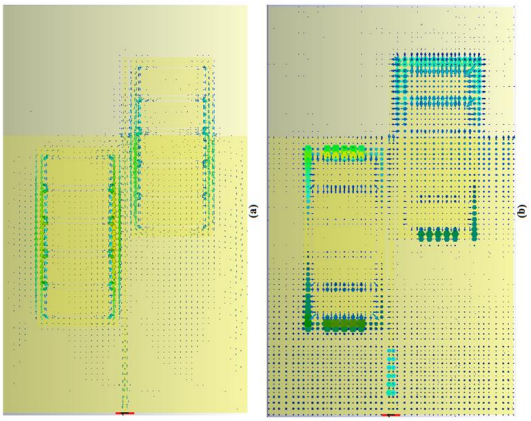

Fig. 10. Current density (a) and electric field (b) density distribution

To design the truncated rings, the principle of the photonic band gap antennas has been applied. The rings follow a proper proportion related to the formulas [61]. Due to reduce the dimensions of the antenna to 30 × 30 mm, the efficiency declined; hence, the thickness of the second layer enhanced to 0.48 mm to compensate for it. By changing the proportion and optimizing the gap, both exact resonance frequency and high efficiency can be achieved. The meshed patch has been refined by cutting a line in the middle of each small rectangular. Then two slot lines with dimensions of: L_t and W_t cut from capacitive part to increase antenna performances and the transparency. Figure 11 shows the final design.

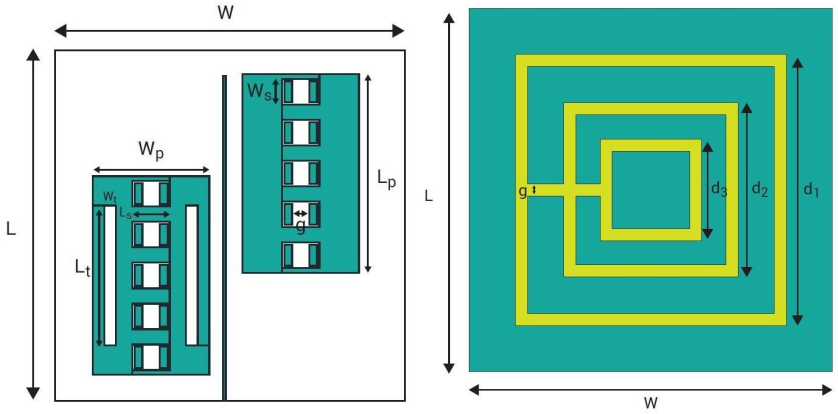

Fig. 11. Antenna geometry (front), (back)

Table 6 show the Antenna geometrical parameters (front)and(back).

Table 6
Antenna geometrical parameters (front)and(back)

Parameters(front)	Dimension(mm)	Parameters(back)	Dimension(mm)
L	30	L	30
W	30	W	30
g	1.5	g	1
W_t	1	d_1	22.4
L_t	12	d_2	14.4
W_p	10	d_3	8.4
L_p	17		
W_s	2.2		
L_s	3.2		

2.6 Proposed Transparent Modified Meshed Antenna Integrated with Solar Cell

Figure 12 shows the perspective view of the simulated proposed transparent modified meshed antenna put together with a solar cell.

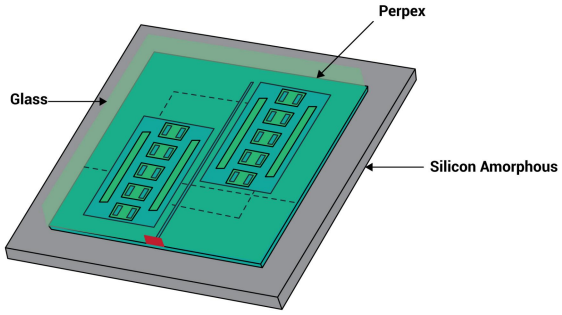

Fig. 12. Perspective view of proposed antenna integrated with solar cell

As seen in this Figure 13, one layer of Perpex [62,63] with the thickness of 3mm and the permittivity of 2.6 [64], has been put on the proposed antenna of the same size. For the solar part, a glass layer with a thickness of 2mm and permittivity of 4.82 and loss tangent of 0.0054, but its size has optimized and increased to get the resonant frequency. Besides, for the metallic part of it, a Silicon Amorphous (the optical) has been chosen. The Perpex was selected because it has a cumulative visible light transmission of 92%. The thin film a-Si solar cells are deposited at the back of the glass substrate. They are 3µm thick and comprise a layered structure composed of a transparent conductive oxide (TCO) front electrode, a p-n silicone junction and an aluminium rear electrode.

3. Result and Discussion

We will present all the simulated results for each of the design steps. The prototyped antenna was designed using Computer Science Technology (CST). It starts by illustrating some antenna sensitivities based on the simulations and fabrication limitations. Then the simulation outcomes of each step for the antenna to finally designed are shown.

3.1 $\lambda/2$ Dimension of Proximity-Fed Cp Antenna

Based on the methodology part after investigating the proper feeding type for the antenna, the polyimide transparent substrate has been chosen because of the cheap price and the availability. Despite being cheap, this substrate has a high loss tangent, which affects our performance. Figure 13 shows the return loss of the antenna resonates at 2.6, 3.5 and the performance can be seen in Table 8.

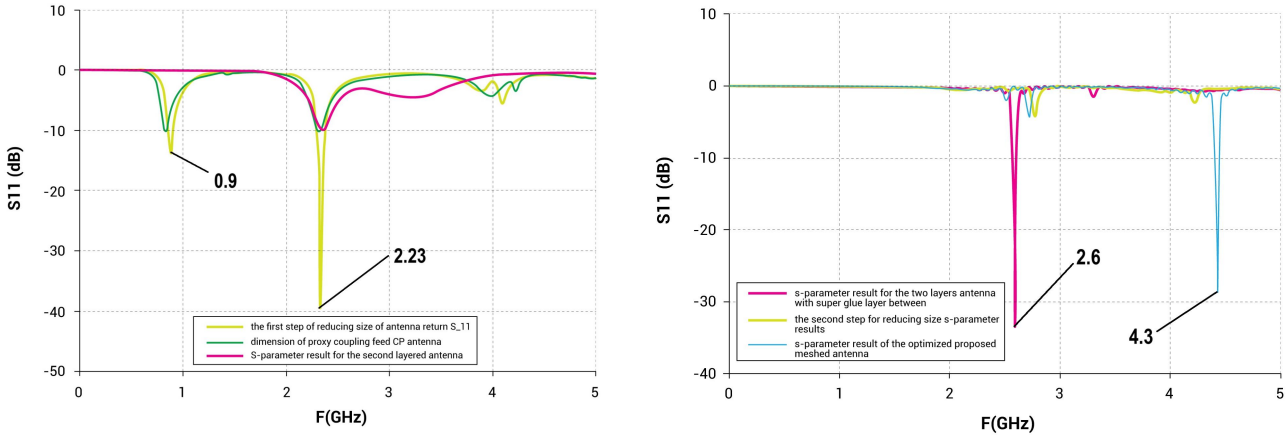

Fig. 13. S-parameter result for the Simulation steps

Table 8
Simulated results of proxy coupling feed CP antenna

Frequency (GHz)	Radiation efficiency (%)	Gain (dBi)
2.6, 3.5	78.35	2.804

As shown in Figure 13, the antenna is resonating at two frequencies, with dimensions still large and radiation efficiency almost high but low gain. To meet application requirements, the antenna dimensions were reduced to a higher frequency and shifted the resonance frequency to a higher frequency band. The S-parameter of the reduced antenna shows a 70% decrease in resonant frequency and 70% increase in radiation efficiency. The dimensions were reduced to λ/4 for the Cap and Ind part of the patch, resulting in a smaller antenna width but still a large length. The second step of reducing S-parameter results in a resonant frequency shift to a higher frequency band, increased radiation efficiency, and a gain of 2.804 dBi.

3.2 The Second Layered Antenna

Afterwards, the antenna dimensions should still decrease to meet the requirement; but this decrement will decrease the performance, especially the radiation efficiency. To compensate for this loss, another layer of tetraethyl substrate has been added to the first one. After adding the second layer together with the ground layer, some sort of mismatch happened between the feeding and antenna because of the improper current distribution caused by the second ground. Figure 14 shows the return loss result for the second layer antenna, which shows the mismatch by showing some small ripples at the other frequencies. Thus, the dimensions should be optimized more to match the resonating frequency. The mismatch is tangible and there is a high back lobe.

Afterwards, by pasting these two layers with a mixture of super glue and air, these defects compensate a bit.

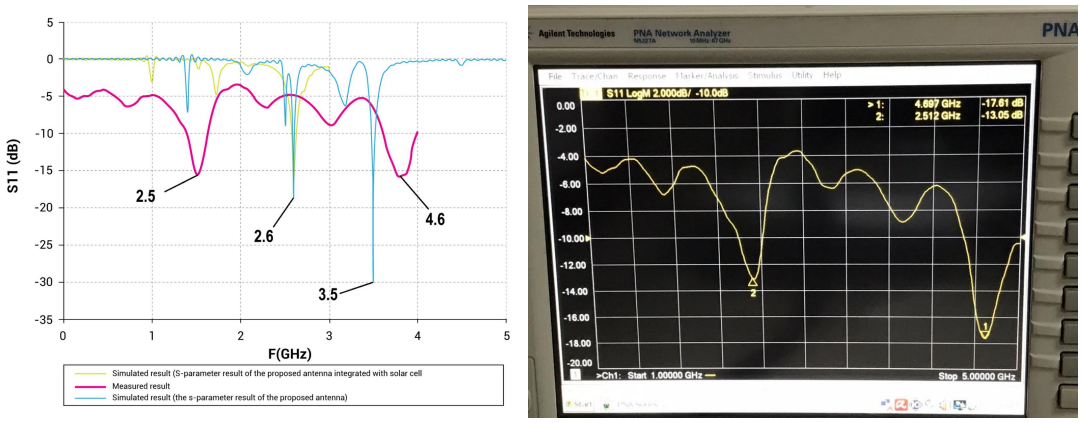

Fig. 14. Simulation and measurement of reflection coefficient result of the proposed antenna, and the antenna integrated with the solar cell

3.3 Optimized Proposed Meshed Antenna

These drawbacks can be fixed by cutting some slots from the second ground layer and cutting the proposed modified meshed from the patch. Figure 13 illustrates s-parameter result of the optimized proposed meshed antenna, which has been cut from the patch. The dimensions of the antenna are 50 × 30 mm now. Figure 15 shows the new antenna with meshed patch's radiation pattern. This radiation pattern is directional, and its direction is in Z- coordinate; while the gain and the radiation efficiency are still low, and they are 1.33 dBi and 33% respectively.

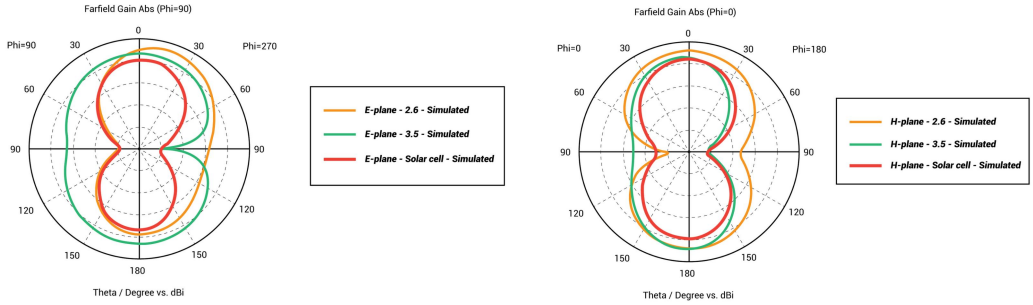

Fig. 15. Proposed antenna simulation radiation pattern, antenna integrated with the solar cell (a) E-plane (b) H-plane

3.4 Proposed Meshed Antenna Results

The first ground layer is optimized for frequency shift and antenna performance by cutting its length in each step. A photonic band gap (PBG) sector with two rectangular sectors and a small square is cut from the second ground. The small squares in the patch are also cut, increasing transparency and performance. The antenna dimensions are optimized, including capacitive distance and photonic band gap proportions. The proposed antenna achieves 3.3 dBi gain and 81.5% radiation efficiency, as shown in Figure 16.

3.5 Proposed Mesh Modified Meshed Antenna Integrate with Solar Cell

Figure 14 shows the S-parameter result of the proposed antenna integrated with solar cell. Based on the S-parameter result, its VSWR there is an excellent match (VSWR= 1.52). The antenna's radiation efficiency has been increased to 83.5% by integration of the solar cell. The gain has been enhanced to 3.8 dBi. With the possibility of exploiting the antenna as an array antenna through the increased number of the element arrays, performing the antenna has the chance to be increased much more. The radiation pattern of the proposed antenna integrated with the solar cell is showed in Figure 15, which is broadside and directed to Z direction. The Simulation result for:

i. Gain
ii. Efficiency
iii. Axial Ratio is showed in Figure 16.

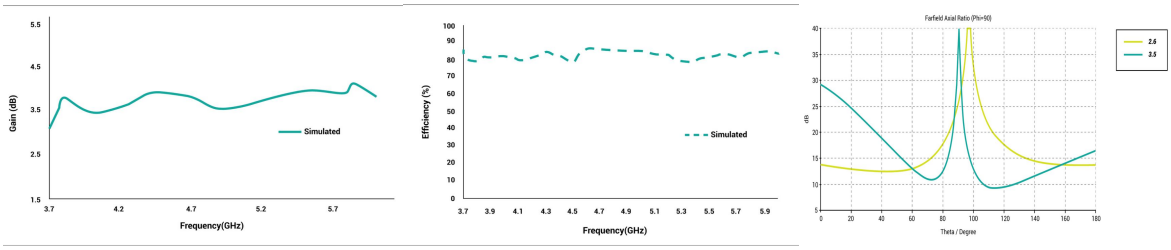

Fig. 16. Simulation result for (a) Gain (b) Efficiency (c) Axial Ratio

After the fabrication, we find the transparency percentage become low 30%, and that because of the limitation of the polyimide flex transparency as we used in the simulation colourless transparent polyimide. however, the antenna size is tiny will not affect the solar cell efficiency too much. Figure 17. Shows the final prototype and the antenna integrate with solar cell.

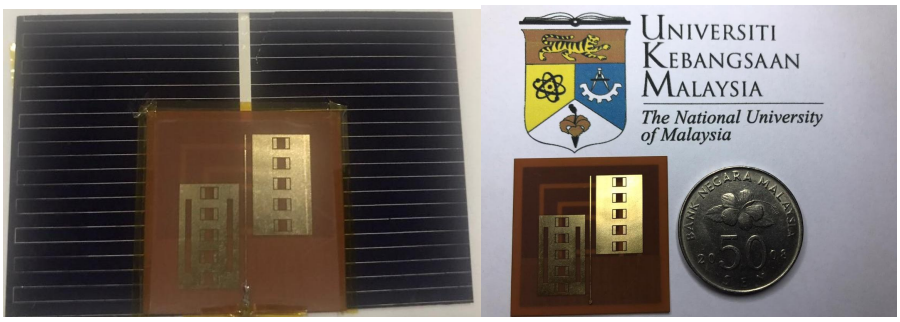

Fig. 17. Proposed fabricated antenna (a) antenna (b) antenna with solar cell

4. Experimental Results

The N5227A PNA Network Analyzer was used to calculate return loss and gain and radiation patterns after fabricated the proposed antenna. The simulated and calculated reflection coefficient graph showed a return loss of 10 dB from 2.6 to 3.5 GHz (30%), with a bandwidth of 2.5 to 4.6 GHz showed in Figure 14. The difference in results was due to dimensional tolerance and difficulties in soldering the SMA to the substrate. To improve efficiency, silicone glue was used to connect the SMA to the substrate and solder the SMA to the antenna transmission line. The efficiency of the antenna can be improved by adding a highly conductive coating near transparent sheets using efficient soldering techniques. The simulated gain is above 3 dBi, and the performance is above 81.5% for the proposed frequency bands.

4.1 Bending Analysis

Flexible smart devices require testing antenna performance under bending conditions, including return loss due to differences in effective electrical length. Simulation methods will be used to measure the coefficient of reflection of the versatile antenna. Figure 18 displays the virtual coefficient of reflection values that clearly illustrate the influence of the structural bending on the frequency of the resonance. Although the measured reflex coefficient suggests deflection from the simulated impact, the antenna still resonates in the band proposed for 5G and WLAN applications.

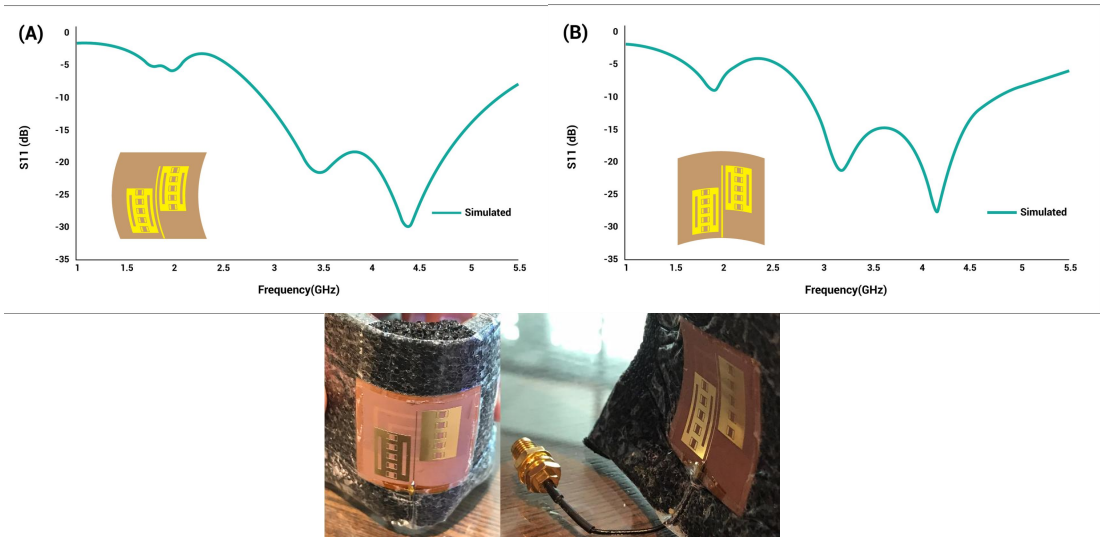

Fig. 18. The Simulation of reflection coefficient when antenna is bent around (a) Y-axis (b) X axis (d) antenna under bending condition

5. Conclusion

As mentioned in this literature, after thorough research of a coplanar proximity feed scheme and substrate materials, it has presented a design of a small mesh antenna with circular polarization. This design will be suited for small satellite applications, reason being it can easily integrate with solar panels of small satellites to spare more surface area. The antenna recommended contains two square meshed patches that are fed with a straight microstrip line, that will then produce two linear polarizations that will be orthogonal in space and quadrature in phase, succeeding to circular polarization. The gain is almost 3.4 dBi, and the efficiency is 81.5 percent, which is reasonable because there are some losses because of meshing and based on the small size of the antenna. The antenna dimensions have been reduced as much as they could compare with the same works in this application. After integrating the proposed antenna with a solar cell, the performances like gain and radiation efficiency increased to 83.5% and 3.48 dBi. Gain and efficiency can be enhanced even more if they have been applied as a bunch of arrays. Few challenges may arise while prototyping this antenna because a good Circular Polarization relies on the coupling of the patches with the feed line that is sensitive to the coupling gaps. Yet, a fabrication that is done carefully with a regular circuit board milling machine can still produce an acceptable outcome. Although this work mainly discussed the use of mesh transparent antennas in solar cells, the application for such antennas is not limited to solar cells on small satellites. These

transparent antennas can be also used in other areas such as windshields of cars and even as transparent RF circuits. This work gives some guidelines and requirements so that antenna engineers and materials scientists can push the boundaries and enable the usage of such materials. Using transparent antenna can enable implementation of transparent RF circuits for aviation, transportation, and consumer electronics. Co-planar coupled feeds can feed materials that are more difficult to bond, such as the feeding of fabric antennas.

Acknowledgements
The authors would like to extend their gratitude to the Centre for Research Instrumentation and Management (CRIM) for their aid, and Universiti Kebangsaan Malaysia (UKM) for the DIP-2018-019 research grant. We would like to thank the Institute of Sustainable Energy (ISE) of Universiti Tenaga Malaysia (UNITEN) for their support through BOLD2025 Program.

References

[1] Simons, Rainee N., and Richard Q. Lee. "Feasibility study of optically transparent microstrip patch antenna." In *International Symposium and Radio Science Meeting*, no. E-10607. 1997.

[2] Alobaidi, Omar Raed, Puvaneswaran Chelvanathan, Sieh Kiong Tiong, Badariah Bais, Md Akhtar Uzzaman, and Nowshad Amin. "Transparent antenna for green communication feature: A systematic review on taxonomy analysis, open challenges, motivations, future directions and recommendations." *IEEE Access* 10 (2020): 12286-12321. https://doi.org/10.1109/ACCESS.2020.3044435

[3] Tung, Phan Duy, and Chang Won Jung. "Optically transparent wideband dipole and patch external antennas using metal mesh for UHD TV applications." *IEEE Transactions on Antennas and Propagation* 68, no. 3 (2019): 1907-1917. https://doi.org/10.1109/TAP.2019.2950077

[4] Lee, Chang Min, Youngsung Kim, Yongjin Kim, Il Kwon Kim, and Chang Won Jung. "A flexible and transparent antenna on a polyamide substrate for laptop computers." *Microwave and Optical Technology Letters* 57, no. 5 (2015): 1038-1042. https://doi.org/10.1002/mop.29011

[5] Al-Samarraay, Mohammed, Omar Al-Zuhairi, Abdullah Hussein Alamoodi, Osamah Shihab Albahri, Muhammet Deveci, Omar Raed Alobaidi, Ahmed Shihab Albahri, and Gang Kou. "An integrated fuzzy multi-measurement decision-making model for selecting optimization techniques of semiconductor materials." *Expert Systems with Applications* 237 (2024): 121439. https://doi.org/10.1016/j.eswa.2023.121439

[6] Stanley, Manoj, Yi Huang, Hanyang Wang, Hai Zhou, Ahmed Alieldin, and Sumin Joseph. "A transparent dual-polarized antenna array for 5G smartphone applications." In *2018 IEEE International Symposium on Antennas and Propagation & USNC/URSI National Radio Science Meeting*, pp. 635-636. IEEE, 2018. https://doi.org/10.1109/APUSNCURSINRSM.2018.8609096

[7] Keriee, Hussam, Mohamad Kamal A. Rahim, Osman Ayop, Nawres Abbas Nayyef, Mustafa Ghanim, O. R. Alobaidi, Bashar Esmail, and Yaqdhan Mahmood Hussein. "A slotted planar antenna for 5G applications." *ELEKTRIKA-Journal of Electrical Engineering* 21, no. 2 (2022): 11-14. https://doi.org/10.11113/elektrika.v21n2.350

[8] Chiu, Chi-Yuk, Shanpu Shen, and Ross D. Murch. "Transparent dual-band antenna for smart watch applications." In *2017 IEEE International symposium on antennas and propagation & USNC/URSI national radio science meeting*, pp. 191-192. IEEE, 2017. https://doi.org/10.1109/APUSNCURSINRSM.2017.8072138

[9] Alobaidi, Omar Raed, Md Akhtaruzzaman, Vidhya Selvanathan, and N. Amin. "Koch fractal loop circular polarization (CP) antenna integrated with solar cells." In *2019 6th International Conference on Space Science and Communication (IconSpace)*, pp. 80-84. IEEE, 2019. https://doi.org/10.1109/IconSpace.2019.8905985

[10] Hasan, AK Mahmud, M. S. Jamal, Nurhifiza Kamaruddin, N. Asim, Kamaruzzaman Sopian, M. D. Akhtaruzzaman, and Omar Raed. "Integration of NiO layer as hole transport material in perovskite solar cells." In *2019 6th International Conference on Space Science and Communication (IconSpace)*, pp. 267-270. IEEE, 2019.

[11] Green, Ryan B., Michelle Guzman, Natalia Izyumskaya, Barkat Ullah, Supapon Hia, Joshua Pitchford, Ranjita Timsina *et al.,* "Optically transparent antennas and filters: A smart city concept to alleviate infrastructure and network capacity challenges." *IEEE Antennas and propagation magazine* 61, no. 3 (2019): 37-47. https://doi.org/10.1109/MAP.2019.2907895

[12] Al-Zuhairi, Omar, Ahmad Shuhaimi, Nafarizal Nayan, Adreen Azman, Anas Kamarudzaman, Omar Alobaidi, Mustafa Ghanim, Estabraq T. Abdullah, and Yong Zhu. "Non-polar gallium nitride for photodetection applications: A systematic review." *Coatings* 12, no. 2 (2022): 275. https://doi.org/10.3390/coatings12020275

[13] Kim, Taehoon, Gwangmook Kim, Hyeohn Kim, Hong-Jib Yoon, Taeseong Kim, Yohan Jun, Tae-Hyun Shin *et al.,* "Megahertz-wave-transmitting conducting polymer electrode for device-to-device integration." *Nature communications* 10, no. 1 (2019): 653. https://doi.org/10.1038/s41467-019-08552-z

[14] Pohl, Cle, and John L. Van Genderen. "Review article multisensor image fusion in remote sensing: concepts, methods and applications." *International journal of remote sensing* 19, no. 5 (1998): 823-854. https://doi.org/10.1080/014311698215748

[15] Ghamisi, Pedram, Behnood Rasti, Naoto Yokoya, Qunming Wang, Bernhard Hofle, Lorenzo Bruzzone, Francesca Bovolo *et al.,* "Multisource and multitemporal data fusion in remote sensing: A comprehensive review of the state of the art." *IEEE Geoscience and Remote Sensing Magazine* 7, no. 1 (2019): 6-39. https://doi.org/10.1109/MGRS.2018.2890023

[16] Podilchak, Symon K., Davide Comite, Brendan K. Montgomery, Yuepei Li, Victoria Gomez-Guillamon Buendia, and Yahia MM Antar. "Solar-panel integrated circularly polarized meshed patch for cubesats and other small satellites." *IEEE Access* 7 (2019): 96560-96566. https://doi.org/10.1109/ACCESS.2019.2928993

[17] Liu, Xinyu, David R. Jackson, Ji Chen, Jingshen Liu, Patrick W. Fink, Gregory Y. Lin, and Nicole Neveu. "Transparent and Nontransparent Microstrip Antennas on a CubeSat: Novel low-profile antennas for CubeSats improve mission reliability." *IEEE Antennas and Propagation Magazine* 59, no. 2 (2017): 59-68. https://doi.org/10.1109/MAP.2017.2655529

[18] Rodriguez, Christian, Henric Boiardt, and Sasan Bolooki. "CubeSat to commercial intersatellite communications: Past, present and future." In *2016 IEEE Aerospace Conference*, pp. 1-15. IEEE, 2016. https://doi.org/10.1109/AERO.2016.7500525

[19] Kaputa, Daniel S., Timothy Bauch, Carson Roberts, Don McKeown, Mark Foote, and Carl Salvaggio. "Mx-1: A new multi-modal remote sensing UAS payload with high accuracy GPS and IMU." In *2019 ieee systems and technologies for remote sensing applications through unmanned aerial systems (stratus)*, pp. 1-4. IEEE, 2019. https://doi.org/10.1109/STRATUS.2019.8713292

[20] Alam, Touhidul, Mohammad Tariqul Islam, Md Amanath Ullah, and Mengu Cho. "A solar panel-integrated modified planner inverted F antenna for low earth orbit remote sensing nanosatellite communication system." *Sensors* 18, no. 8 (2018): 2480. https://doi.org/10.3390/s18082480

[21] Al-Hiti, Ahmed Shakir, and O. R. Alobaidi. "High energy, dual-wavelength Q-switched Er-doped fiber laser by Ga: ZnO nanoparticle saturable absorber." *Optical Fiber Technology* 87 (2024): 103931. https://doi.org/10.1016/j.yofte.2024.103931

[22] Tawk, Youssef, Joseph Costantine, Firas Ayoub, and Christos G. Christodoulou. "A communicating antenna array with a dual-energy harvesting functionality [wireless corner]." *IEEE Antennas and Propagation Magazine* 60, no. 2 (2018): 132-144. https://doi.org/10.1109/MAP.2018.2796025

[23] Rashidian, Atabak, Lotfollah Shafai, and Cyrus Shafai. "Miniaturized transparent metallodielectric resonator antennas integrated with amorphous silicon solar cells." *IEEE Transactions on Antennas and Propagation* 65, no. 5 (2017): 2265-2275. https://doi.org/10.1109/TAP.2017.2679492

[24] Lemey, Sam, Sam Agneessens, Patrick Van Torre, Kristof Baes, Jan Vanfleteren, and Hendrik Rogier. "Wearable flexible lightweight modular RFID tag with integrated energy harvester." *IEEE Transactions on Microwave Theory and Techniques* 64, no. 7 (2016): 2304-2314. https://doi.org/10.1109/TMTT.2016.2573274

[25] Zhang, Yujie, Shanpu Shen, Chi Yuk Chiu, and Ross Murch. "Hybrid RF-solar energy harvesting systems utilizing transparent multiport micromeshed antennas." *IEEE Transactions on Microwave Theory and Techniques* 67, no. 11 (2019): 4534-4546. https://doi.org/10.1109/TMTT.2019.2930507

[26] O'Conchubhair, Oisin, Patrick McEvoy, and Max J. Ammann. "Integration of antenna array with multicrystalline silicon solar cell." *IEEE Antennas and Wireless Propagation Letters* 14 (2015): 1231-1234. https://doi.org/10.1109/LAWP.2015.2399652

[27] Sheikh, Shahin, Mehrdad Shokooh-Saremi, and Mohammad-Mehdi Bagheri-Mohagheghi. "Transparent microstrip patch antenna based on fluorine-doped tin oxide deposited by spray pyrolysis technique." *IET Microwaves, Antennas & Propagation* 9, no. 11 (2015): 1221-1229. https://doi.org/10.1049/iet-map.2015.0048

[28] Al-Adhami, Yasir, and Ergun Erçelebi. "Plasmonic metamaterial dipole antenna array circuitry based on flexible solar cell panel for self-powered wireless systems." *Microwave and Optical Technology Letters* 59, no. 9 (2017): 2365-2371. https://doi.org/10.1002/mop.30747

[29] An, Wenxing, Lin Xiong, Shenheng Xu, Fan Yang, Hai-Peng Fu, and Jian-Guo Ma. "A Ka-band high-efficiency transparent reflectarray antenna integrated with solar cells." *IEEE Access* 6 (2018): 60843-60851. https://doi.org/10.1109/ACCESS.2018.2875359

[30] Moharram, Mohamed A., and Ahmed A. Kishk. "Optically transparent reflectarray antenna design integrated with solar cells." *IEEE Transactions on Antennas and Propagation* 64, no. 5 (2016): 1700-1712. https://doi.org/10.1109/TAP.2016.2539379

[31] Alhasan, Ameer, Lukman Audah, Mohammed Hasan Alwan, and O. R. Alobaidi. "An energy aware qos trust model for energy consumption enhancement based on clusters for IoT networks." *Journal of Engineering Science and Technology* 16, no. 2 (2021): 968-987.
[32] Yasin, Tursunjan, and Reyhan Baktur. "Bandwidth enhancement of meshed patch antennas through proximity coupling." *IEEE Antennas and Wireless Propagation Letters* 16 (2017): 2501-2504. https://doi.org/10.1109/LAWP.2017.2726562
[33] Yekan, Taha, and Reyhan Baktur. "Conformal integrated solar panel antennas: Two effective integration methods of antennas with solar cells." *IEEE Antennas and Propagation Magazine* 59, no. 2 (2017): 69-78. https://doi.org/10.1109/MAP.2017.2655577
[34] Sheikh, Shahin. "Circularly polarized meshed patch antenna." *IEEE Antennas and Wireless Propagation Letters* 15 (2015): 352-355. https://doi.org/10.1109/LAWP.2015.2445836
[35] Kocia, Catherine, and Sean Victor Hum. "Design of an optically transparent reflectarray for solar applications using indium tin oxide." *IEEE Transactions on antennas and Propagation* 64, no. 7 (2016): 2884-2893. https://doi.org/10.1109/TAP.2016.2555338
[36] Xi, Baoliang, Xianling Liang, Qian Chen, Kun Wang, Junping Geng, and Ronghong Jin. "Optical transparent antenna array integrated with solar cell." *IEEE Antennas and Wireless Propagation Letters* 19, no. 3 (2020): 457-461. https://doi.org/10.1109/LAWP.2020.2969694
[37] Jaakkola, Kaarle, and Kirsi Tappura. "Exploitation of transparent conductive oxides in the implementation of a window-integrated wireless sensor node." *IEEE Sensors Journal* 18, no. 17 (2018): 7193-7202. https://doi.org/10.1109/JSEN.2018.2852561
[38] Al-Shalaby, Noha A., and Shaymaa M. Gaber. "Parametric study on effect of solar-cell position on the performance of transparent DRA transmitarray." *AEU-International Journal of Electronics and Communications* 70, no. 4 (2016): 436-441. https://doi.org/10.1016/j.aeue.2016.01.006
[39] Cai, Longzhu. "An on-glass optically transparent monopole antenna with ultrawide bandwidth for solar energy harvesting." *electronics* 8, no. 9 (2019): 916. https://doi.org/10.3390/electronics8090916
[40] Ta, Son Xuat, Jae Jin Lee, and Ikmo Park. "Solar-cell metasurface-integrated circularly polarized antenna with 100% insolation." *IEEE Antennas and Wireless Propagation Letters* 16 (2017): 2675-2678. https://doi.org/10.1109/LAWP.2017.2740570
[41] Jones, Thomas R., John P. Grey, and Mojgan Daneshmand. "Solar panel integrated circular polarized aperture-coupled patch antenna for CubeSat applications." *IEEE Antennas and Wireless Propagation Letters* 17, no. 10 (2018): 1895-1899. https://doi.org/10.1109/LAWP.2018.2869321
[42] Haraty, Mohammad Reza, Mohammad Naser-Moghadasi, Abbas Ali Lotfi-Neyestanak, and Alireza Nikfarjam. "Transparent flexible antenna for UWB applications." *The Applied Computational Electromagnetics Society Journal (ACES)* (2016): 1426-1430.
[43] Zarbakhsh, Saman, Mohammad Akbari, Mohammadmahdi Farahani, Alireza Ghayekhloo, Tayeb A. Denidni, and Abdel-Razik Sebak. "Optically transparent subarray antenna based on solar panel for CubeSat application." *IEEE Transactions on Antennas and Propagation* 68, no. 1 (2019): 319-328. https://doi.org/10.1109/TAP.2019.2938740
[44] Zarbakhsh, Saman, Mohammad Akbari, Fereshteh Samadi, and Abdel-Razik Sebak. "Broadband and high-gain circularly-polarized antenna with low RCS." *IEEE Transactions on Antennas and Propagation* 67, no. 1 (2018): 16-23. https://doi.org/10.1109/TAP.2018.2876234
[45] An, Wenxing, Shenheng Xu, Fan Yang, and Jianfeng Gao. "A Ka-band reflectarray antenna integrated with solar cells." *IEEE Transactions on Antennas and Propagation* 62, no. 11 (2014): 5539-5546. https://doi.org/10.1109/TAP.2014.2354424
[46] An, Wenxing, Lin Xiong, Shenheng Xu, Fan Yang, Hai-Peng Fu, and Jian-Guo Ma. "A Ka-band high-efficiency transparent reflectarray antenna integrated with solar cells." *IEEE Access* 6 (2018): 60843-60851. https://doi.org/10.1109/ACCESS.2018.2875359
[47] Kang, Seok Hyon, and Chang Won Jung. "Transparent patch antenna using metal mesh." *IEEE Transactions on Antennas and Propagation* 66, no. 4 (2018): 2095-2100. https://doi.org/10.1109/TAP.2018.2804622
[48] Hautcoeur, Julien, Larbi Talbi, Khelifa Hettak, and Mourad Nedil. "60 GHz optically transparent microstrip antenna made of meshed AuGL material." *IET Microwaves, Antennas & Propagation* 8, no. 13 (2014): 1091-1096. https://doi.org/10.1049/iet-map.2013.0564
[49] Arellano, Jesus A. *Inkjet-printed highly transparent solar cell antennas*. Utah State University, 2011.
[50] Martin, Alexis, Olivier Lafond, Mohamed Himdi, and Xavier Castel. "Improvement of 60 GHz transparent patch antenna array performance through specific double-sided micrometric mesh metal technology." *Ieee Access* 7 (2018): 2256-2262. https://doi.org/10.1109/ACCESS.2018.2886478

[51] Alobaidi, O. R., P. Chelvanathan, B. Bais, K. Sopian, M. A. Alghoul, Md Akhtaruzzaman, and N. Amin. "Vacuum annealed Ga: ZnO (GZO) thin films for solar cell integrated transparent antenna application." *Materials Letters* 304 (2021): 130551. https://doi.org/10.1016/j.matlet.2021.130551

[52] Ain, M. F., M. Y. Qasaymeh, Z. A. Ahmad, M. A. Zakariya, and Ubai Ullah. "An equivalent circuit of microstrip slot coupled rectangular dielectric resonator antenna." (2012).

[53] Outaleb, N., J. Pinel, M. Drissi, and O. Bonnaud. "Microwave planar antenna with RF-sputtered indium tin oxide films." *Microwave and Optical Technology Letters* 24, no. 1 (2000): 3-7. https://doi.org/10.1002/(SICI)1098-2760(20000105)24:1<3::AID-MOP2>3.3.CO;2-8

[54] Miyazaki, Toshiyuki. "Analysis and design on a proximity fed microstrip antenna." *IEICE Proceedings Series* 8, no. POS-A3-5 (1996).

[55] Jha, Kumud Ranjan, and Ghanshyam Singh. "Dual-band rectangular microstrip patch antenna at terahertz frequency for surveillance system." *Journal of computational electronics* 9 (2010): 31-41. https://doi.org/10.1007/s10825-009-0297-8

[56] Sharma, Aditi, Vivek K. Dwivedi, and G. Singh. "THz rectangular microstrip patch antenna on multilayered substrate for advance wireless communication systems." In *Progress in electromagnetics research symposium, Beijing, China*, pp. 627-631. 2009.

[57] Azarbar, Ali, M. S. Masouleh, and A. K. Behbahani. "A new terahertz microstrip rectangular patch array antenna." *International Journal of Electromagnetics and Applications* 4, no. 1 (2014): 25-29.

[58] Pozar, David M., and Daniel H. Schaubert. "The analysis and design of microstrip antennas and arrays." *A Selected Reprint Volume. IEEE Antennas and Propagation Society Sponsor. New York* (1995). https://doi.org/10.1109/9780470545270

[59] Raje, S., S. Kazemi, and H. R. Hassani. "Wideband stacked koch fractal antenna with H-Shape aperture coupled feed." In *2007 Asia-Pacific Microwave Conference*, pp. 1-4. IEEE, 2007. https://doi.org/10.1109/APMC.2007.4554915

[60] Thilagam, Salai Thillai. "Design and comparison of microstrip slot antennas." (2011).

[61] Karmakar, Nemai Chandra, and Mohammad Nurunnabi Mollah. "Investigations into nonuniform photonic-bandgap microstripline low-pass filters." *IEEE Transactions on microwave theory and techniques* 51, no. 2 (2003): 564-572. https://doi.org/10.1109/TMTT.2002.807817

[62] Dunsky, Corey M., and Finlay Colville. "Application report-Scribing thin-film solar panels-Process and laser optimization are key for high throughput and precise clean scribes." *Industrial Laser Solutions for Manufacturing* 23, no. 2 (2008): 16.

[63] Poortmans, Jef, and Vladimir Arkhipov, eds. *Thin film solar cells: fabrication, characterization and applications*. Vol. 18. John Wiley & Sons, 2006. https://doi.org/10.1002/0470091282

[64] Roo Ons, Maria Jose. "Integration of antennas and solar cells for autonomous communication systems." (2010).